

# Groundwater Quality Assessment and Irrigation Suitability for Agricultural Use in Charnockite–Migmatite Terrains of Southern India

Pragadeeshwaran Kannan<sup>1\*</sup>; Gurugnanam Balasubramaniyan<sup>\*1</sup>, Bairavi Swaminathan<sup>1</sup>; Bagyaraj Murugesan<sup>1</sup>, Suresh M

<sup>1</sup>Centre for Applied Geology, The Gandhigram Rural Institute (Deemed to be University), Gandhigram, Dindigul-624302, Tamil Nadu, India. (PK: pragadeeshpragadeesh2204@gmail.com; Orcid id - <https://orcid.org/0009-0009-0387-4348> ; GB: gurugis4u@gmail.com, Orcid id <https://orcid.org/0000-0002-8775-7123> ; BS: bairuguru98@gmail.com; BM: geobagya25@gmail.com, Orcid id - <https://orcid.org/0000-0002-3076-8884> )

<sup>2</sup>Department of Geology, Rani Anna College for Women, Tirunelveli - 627 008 (MS- watersuresh@gmail.com)

---

## ABSTRACT

Groundwater is a vital source for human life to survive and fulfil the needs for both drinking and irrigation purposes in the Alamarathupatti region of Dindigul district, Tamil Nadu, India. This research aims to evaluate the groundwater suitability for drinking and irrigation with 20 groundwater samples collected around the study region and analysed the physicochemical parameters using standard methods. pH, TDS, EC, TH, Ca<sup>2+</sup>, Mg<sup>2+</sup>, Na<sup>+</sup>, K<sup>+</sup>, Cl<sup>-</sup>, HCO<sub>3</sub><sup>-</sup>, and SO<sub>4</sub><sup>2-</sup> exceeding permissible limits. Spatial distribution was mapped using Inverse Distance Weighting (IDW). The Piper interpretation indicates that the water type is Ca<sup>2+</sup>-Mg<sup>2+</sup>-Cl-SO<sub>4</sub><sup>2-</sup>, indicating ion exchange and anthropogenic influence. Gibbs suggests rock dominance is the primary factor affecting groundwater chemistry. In Irrigation suitability, Wilcox's interpretation indicates that most samples fall in the Good to Permissible category. The GWQI indicates that 95% samples fall in poor water, suggesting groundwater is generally unsuitable for direct consumption without treatment and 5 % in Good category. Correlation analysis revealed strong relationships among EC, TDS, hardness, and major ions, indicating rock–water interaction and ionic enrichment in the groundwater system. Principal component analysis explicates 55.34% total variance and the major component is PC 1, explaining 30.90% indicates rock-water interaction and anthropogenic activities.

**Keywords:** Hydrogeochemistry; Water Quality Index; PCA; Piper diagram; Irrigation suitability.

---

## 1. INTRODUCTION

Groundwater plays a crucial role in sustaining agricultural, industrial, and domestic sectors, especially in southern India's semi-arid and hard rock terrains. The quality and sustainability of groundwater resources are under growing pressure due to rapid urbanization, over-extraction, and geogenic and anthropogenic pollution (Subramani et al., 2005). In regions underlain by charnockite and migmatite formations, the hydrochemistry of groundwater is primarily influenced by rock-water interactions, particularly during weathering of feldspar and pyroxene-bearing silicates that elevate ionic concentrations in groundwater (Duraismy et al., 2019).

Hydrochemical evaluation using statistical and spatial tools is essential to delineate groundwater's geochemical evolution and irrigation suitability (Panneerselvam et al., 2020). Studies (Rajmohan & Elango, 2006) have emphasised that mapping spatial patterns of major ions and water quality indices such as the Groundwater Quality Index (GWQI) is critical for understanding aquifer vulnerability and guiding water resource planning. Recent assessments by (Karunanidhi, Aravinthasamy, Deepali, et al., 2020) also highlight the integration of multivariate statistical approaches with hydrochemical diagrams such as Piper, Gibbs and Wilcox plots to classify water types, identify dominant geochemical factors, and evaluate their suitability for drinking and irrigation purposes. Principal Component Analysis (PCA) is widely used in hydrogeochemical studies and to identify the processes affecting groundwater composition like anthropogenic factors, mineral dissolution by converting complex datasets into a restricted number of interpretable components (Wang et al., 2022). In this context, the present study focuses on hydrogeochemical characterization of groundwater in Alamarathupatti regions, located in Athoor Taluk, Dindigul District, Tamil Nadu. Post-monsoon groundwater samples were analyzed and interpreted using graphical tools and spatial interpolation to assess their potability and irrigation usability. This

study is the first detailed hydrogeochemical assessment of the Alamarathupatti region, integrating spatial mapping and multivariate statistics to distinguish geogenic processes from anthropogenic influences.

## 2. STUDY AREA

The Alamarathupatti region is located in the Athoor taluk, and it is 8 kilometres from Dindigul town. The latitude and longitude extensions are 10°18'30"- 10°19'30"N and 77°55'30" - 77°57'0"E as shown in Fig. 1. In summer months April to June the temperature varies from 27 - 39°C and November to January with temperature of 22 - 31°C. The study area comprises migmatite and charnockite gneiss complexes. High-grade metamorphic rocks like charnockite are usually abundant in feldspar, quartz, and pyroxene.

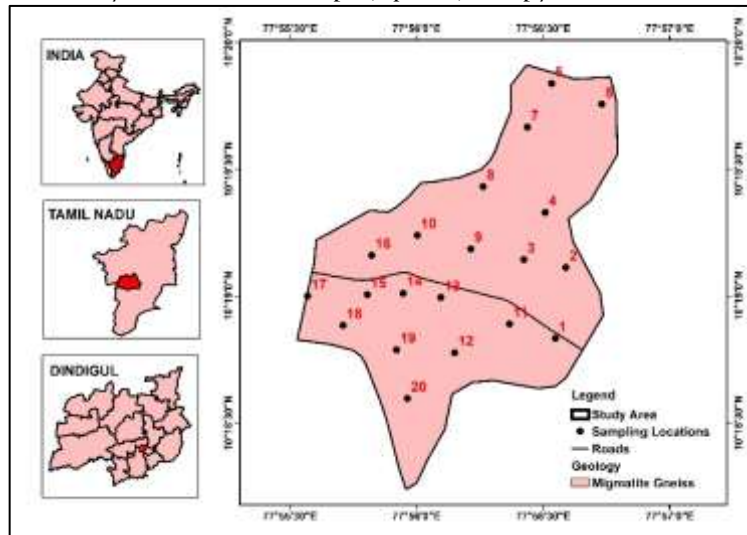


Fig. 1 Study area map

## 3. METHODOLOGY

### 3.1 Groundwater sampling methods

Groundwater samples were collected during the post-monsoon season 2023 to evaluate physicochemical parameters. About 20 groundwater samples were obtained from the borewells. All samples were obtained with 1 L bottles. The polypropylene bottles were washed 2 to 3 times with HNO<sub>3</sub> to prevent contamination. The wells were driven for about 5–10 minutes before sample collection to restrict influence of the pipe. pH, TDS, EC was analysed in the field with handheld instruments (pH - (Pen type) (ECO) pH TEST 1-EUTECH 01X460901, TDS & EC- TDS meter (Pen type) (ECO) TDS TEST- EUTECH). Groundwater sample bottles were tightly sealed, transported to the laboratory, and examined after storage at 4°C. Standard recommended techniques were used to explore physical and chemical parameters such as Ca<sup>2+</sup>, Mg<sup>2+</sup>, Cl<sup>-</sup>, CO<sub>3</sub><sup>2-</sup> and HCO<sub>3</sub><sup>-</sup> levels, which were examined using volumetric titration (APHA, 2017). A flame photometer (Elico CL0378) and spectrometer (Elico SL 207 mini) were used to determine Na<sup>+</sup>, K<sup>+</sup>, and SO<sub>4</sub><sup>2-</sup> concentrations. Fluoride was analysed using a fluorimeter (Thermo Orion star A214 series pH/ISE benchtop meter kit), and nitrate was analysed using a nitrate electrode meter (Lmion-40). The total hardness of CaCO<sub>3</sub> was calculated using the following equation (1):

$$TH = 2.497 \times [Ca^{2+}] + 4.118 \times [Mg^{2+}] \quad (1)$$

The calculated ionic balance error is within the desirable range of ± 10%, as shown in equation (2):

$$IBE (\%) = \{(\Sigma Cations - \Sigma Anions) / (\Sigma Cations + \Sigma Anions)\} \times 100 \quad (2)$$

### 3.2 Groundwater Water Quality Index (GWQI)

The groundwater quality index was calculated using the weighted arithmetic index method to evaluate water quality (Tyagi et al., 2013). This is the easiest and most accurate method for calculating the water quality index for a particular location, as shown in Eqs. 3-6.

For each parameter, the relative weight (Wi) was calculated using Eq.3 below:

$$W_i = w_i / \sum_{i=1}^n w_i \quad (3)$$

The quality rating (qi) for each parameter was determined using Eq.4, the formula:

$$Q_i = (V_i - V\{ideal\}) / V\{standard\} - V\{ideal\} \times 100 \quad (4)$$

" $V_i$  is the parameter's observed value", " $V_{ideal}$  is the parameter's ideal value", and  $V_{Standard}$  (WHO,2017) is permissible value of parameter. Each parameter is given a relative weight ( $W_i$ ). The formula used to calculate the subindex ( $S_i$ ) of each parameter is as follows: Eq.5:

$$S_i = W_i \times q_i \quad (5)$$

The WQI is obtained by all sub-indices, and calculated using Eq.6, is as follows :

$$WQI = \sum S_i / \sum W_i \quad (6)$$

$\sum W_i$  is obtained by adding the sum of all the calculated relative weights, and  $\sum S_i$  is sum of all calculated sub-indices. The WQI is classified into "Excellent < 50, Good 50 -100, Poor 100 – 200, Very Poor 200 – 300, and unsuitable for drinking > 300" to evaluate water quality (Ahirvar et al., 2023).

### 3.3 Spatial distribution map using inverse distance weighting method

The IDW method is generally used for spatial interpolation to assess environmental factors like air quality, groundwater pollution, and contaminant distribution. IDW works by estimating values at unmeasured locations based on the known values' proximity, with closer points receiving higher weights (Choi & Chong, 2022). This method has proven effective in mapping pollutants and evaluating their possible impacts on society's health and the surroundings. (Stachelek & Madden, 2015) Introduced an enhanced version of IDW called inverse path distance weighting (IPDW), which improves spatial mapping accuracy by accounting for barriers like peninsulas and islands in coastal water quality studies.

### 3.4 Statistical analysis

A complete statistical evaluation of the groundwater characteristics Minimum, Maximum, mean, and standard deviation provided a complete range . SPSS multivariate techniques, like Pearson's correlation and Principal Component Analysis using the factor analysis method, were used to evaluate the correlations between each parameter. It is used to identify trends in different groundwater quality parameters, and the values 1 or -1 indicate positive and negative correlations, respectively. These helps identify the significant factors affecting groundwater quality.

## 4. RESULTS AND DISCUSSION

The table below shows complete results of statistical outlines for the groundwater quality parameters

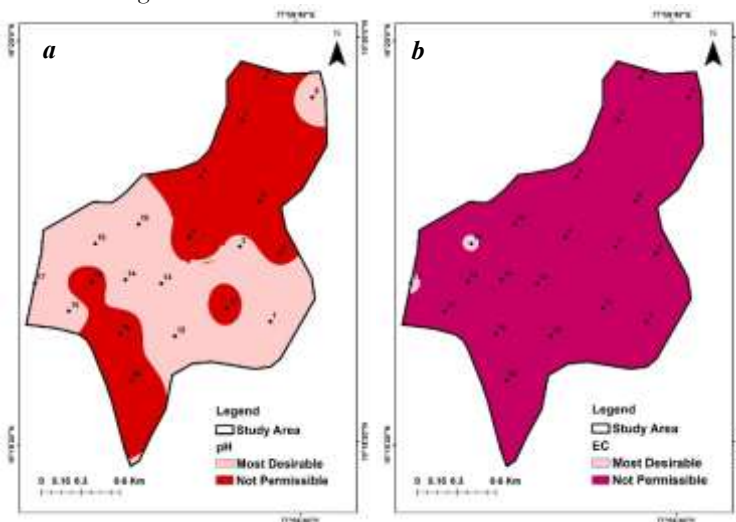
**Table 1 presents the statistical outlines of the groundwater quality parameters**

Parameters	Min	Max	Mean	Std Dev	Skewness	Kurtosis	Median	(WHO, 2017)		% of Samples Exceed the Limit
								Most Desirable	Not Permissible	
pH	8.08	8.85	8.50	0.22	-0.38	-0.69	8.50	6.5-8.5	<6.5 and >8.5	55
EC (µS/cm)	1272.00	4204.00	2273.80	682.83	1.03	2.05	2137.00	<1500	>1500	90
TDS (mg/L)	631.00	2092.00	1130.40	339.87	1.03	2.08	1072.00	<500	>1500	100
TH (mg/L)	335.20	1835	870.51	386.07	0.29	1.50	852.50	<100	>500	100
Ca <sup>2+</sup> (mg/L)	76.0	214	111.01	34.93	1.82	3.40	102.10	<75	>200	5
Mg <sup>2+</sup> (mg/L)	60.70	315.90	150.23	68.69	0.59	-0.04	151.26	<50	>150	50
Na <sup>+</sup> (mg/L)	11.00	276.10	137.28	56.64	0.08	1.26	146.90	<200	>200	5
K <sup>+</sup> (mg/L)	68.90	89.10	80.10	6.92	-0.24	-1.38	80.50	<10	>10	100

Cl <sup>-</sup> (mg/L)	132.9 3	109 0.08	361.1 4	227.3 2	2.28	5.51	288.03	<250	>250	5
NO <sub>3</sub> <sup>-</sup> (mg/L)	5.00	30.0 0	13.00	6.96	0.68	0.05	10.00	<45	>45	0
SO <sub>4</sub> <sup>2-</sup> (mg/L)	124.0 0	590. 00	362.6 0	151.3 6	-0.05	-1.31	377.50	<400	>400	25
HCO <sub>3</sub> <sup>-</sup> (mg/L)	207.4 0	176 9.00	702.6 2	312.0 8	1.90	7.27	674.05	<300	>600	75

#### 4.1 Physical parameters

The pH varied from 8.08 to 8.85, indicating that 55% of samples exceed the most desirable limit (Table 1). These are due to the geogenic processes common in migmatite terrains, where the weathering of silicate minerals occurs, and the release of alkali metals elevates the pH levels (Adimalla & Qian, 2019). pH spatial map is shown in Fig. 2a. EC values ranges from 1272 to 4204  $\mu$ S/cm, indicating that 90% of samples exceeded the most desirable limit (Table 1). The study area's groundwater is naturally enriched with high mineral content, such as Calcium, Magnesium, sodium, and bicarbonate, contributing to high EC values. These are more common in arid and semiarid regions, where aquifers are mineral-rich. EC spatial map is shown in Fig. 2b. The Total dissolved solids ranged from 631 - 2092 (mg/L), resulting in 100% samples exceed the most desirable limit (Table 1). The study area primarily depends on agricultural practices; fertilisers used in crops reach agricultural runoff, and they often contain pesticides and salts that elevate the levels of TDS in neighbouring water bodies and affect subsurface groundwater quality (Panneerselvam et al., 2023). Prolonged consumption of water with high TDS levels can lead to the formation of kidney stones, hypertension, and cardiovascular diseases. TDS spatial map is shown in Fig. 2c. The Total hardness varies from 335 - 1835 (mg/L), indicating that 100% samples exceed the most desirable limit (Table 1). As this study area is an overexploited zone, the decrease in groundwater levels leads to an elevated concentration of dissolved minerals, such as Calcium and Magnesium, contributing to increased hardness. Charnockite and migmatite undergo weathering and release minerals into groundwater. Although a hard rock terrain, it commonly contributes to high groundwater hardness ((CGWB), 2024). TH spatial map is shown in Fig. 2d.



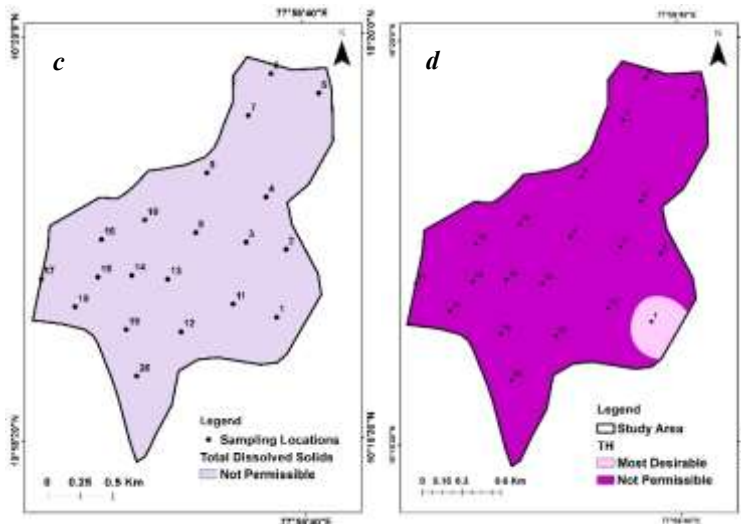
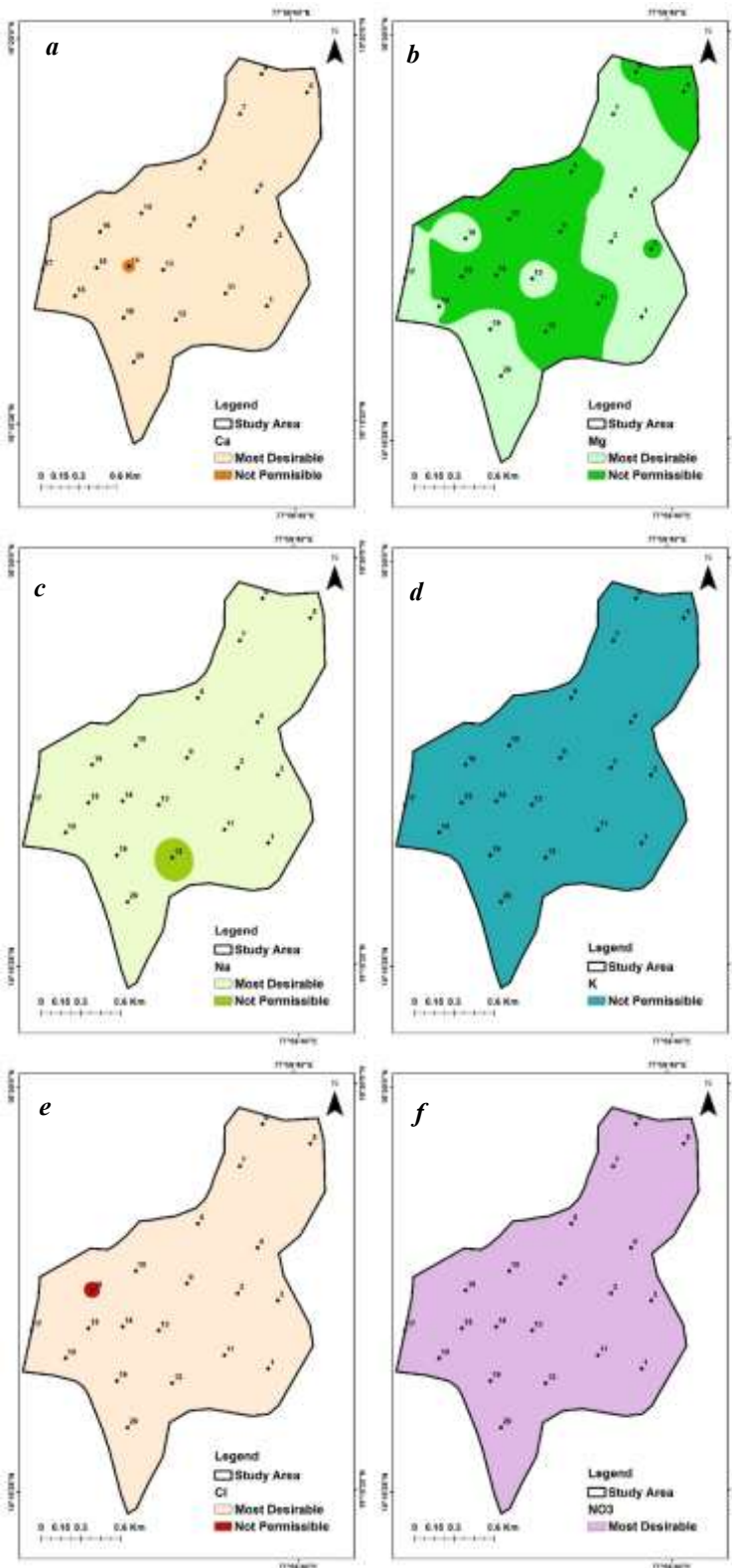


Fig. 2 Spatial Maps a) pH, b) EC, c) TDS, d) TH

#### 4.2 Chemical parameters

The calcium content varied from 76 to 214 (mg/L), indicating that 5% samples exceeds the most desirable limit (Table 1). The excess calcium is due to the weathering of charnockite and migmatite rocks, rich in minerals such as feldspar and pyroxene (Adithya et al., 2016). Because of the natural rock-water interaction, these release calcium ions into the water. Continuous consumption of calcium-rich water causes health issues, such as gastrointestinal issues, kidney disease, and corrosion in water supply pipes (Subramaniyan et al., 2024). Calcium spatial map is shown in Fig. 3a. The magnesium content varied from 60 - 315 (mg/L), indicating that 50% samples exceeds the most desirable limit (Table 1). Charnockite and migmatite are metamorphic rocks rich in silicate minerals that contain high amounts of magnesium-bearing minerals such as pyroxene and amphibole. Magnesium spatial map is shown in Fig.3b. Sodium varied from 11 - 276 (mg/L), indicates that 5% samples exceed the most desirable limit (Table 1). The charnockite and migmatite terrains are rich in silicate minerals, such as feldspar and amphibole. These contain significant amounts of sodium-bearing minerals, and chemical weathering releases sodium ions into the groundwater (Upendra et al., 2022). Sodium spatial map is shown in Fig. 3c. The potassium varied from 68 to 89 (mg/L), indicating that 100% of samples exceed the most desirable limit (Table 1). The elevated potassium concentrations are due to the natural weathering of K-bearing silicates, such as micas and feldspar, and anthropogenic influences, such as using potassium-rich fertilisers. Similar studies have been conducted in other hard-rock terrains in South India (Rajmohan & Elango, 2005). Potassium spatial map is shown in Fig. 3d. The chloride varied from 132 to 1090 (mg/L), indicating that 5% samples exceeds the most desirable limit (Table 1). The geological source of increasing chloride levels is the mineral weathering of charnockite and migmatite, which is significantly smaller than the anthropogenic source; however, it adds up to an overall amount. Chloride spatial map is shown in Fig. 3e.

The nitrate concentration ranges from 5 - 30 (mg/L), indicating that none of samples exceed the most desirable level (Table 1). Nitrate spatial map is shown in Fig. 3f. The sulphate concentration varies from 124 - 590 (mg/L), indicating that 25% of samples exceed the most desirable limit (Table 1). Charnockite and migmatite terrains often contain accessory sulphide minerals like pyrite ( $\text{FeS}_2$ ) and chalcopryrite, especially along fracture zones. The oxidation of these minerals during water-rock interactions can release sulphate into groundwater (Rajmohan & Elango, 2005). Sulphate spatial map is shown in Fig. 3g. The bicarbonate varied from 207 to 1769 (mg/L), 75% samples exceeding the most desirable limit (Table 1). Discharging wastewater and partially treated water due to urbanisation and industrial activities elevates the bicarbonate levels. Spatial map is shown in Fig. 3h.



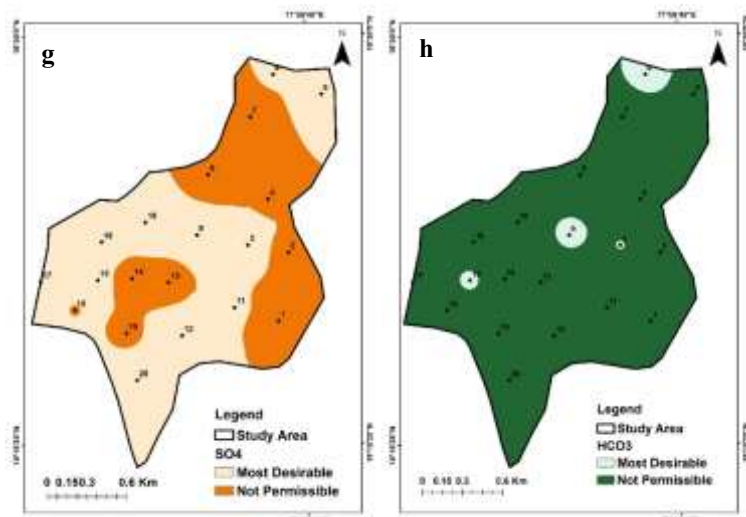


Fig. 3 Spatial Maps a)  $\text{Ca}^{2+}$ , b)  $\text{Mg}^{2+}$ , c)  $\text{Na}^+$ , d)  $\text{K}^+$ , e)  $\text{Cl}^-$ , f)  $\text{NO}_3^-$ , g)  $\text{SO}_4^{2-}$ , h)  $\text{HCO}_3^-$

#### 4.3 Comparison with Other Hard Rock Aquifers

The hydrogeochemical characteristics of the Alamarathupatti region is aligned with similar studies in other hard rock aquifers across peninsular India. For example, (Duraisamy et al., 2019) reported similar  $\text{Ca}^{2+}$ - $\text{Mg}^{2+}$ - $\text{Cl}^-$  type water with elevated TDS and EC in the Kangayam region of Tamil Nadu, highlighting the influence of silicate weathering and anthropogenic sources. (Adimalla & Qian, 2019) Comparable geochemical parameters were observed in hard rock terrain of Telangana, where fluoride and bicarbonate levels were high due to prolonged rock-water interactions. Likewise, (Upendra et al., 2022) reported elevated salinity and  $\text{Ca}^{2+}$ - $\text{Na}^+$ - $\text{Cl}^-$  water type dominance in the Cauvery River basin. These findings indicate that the geochemical processes affecting the Alamarathupatti aquifer are not site-specific but are regionally prevalent across charnockite and migmatite-dominated crystalline terrains. Incorporating these comparative insights broadens the applicability of the study and positions it within a larger hydrogeological context, which is essential for framing regional-wide groundwater management strategies.

### 5. INTERPRETATION

#### 5.1 Piper plot

The Piper plot indicates that in cation, majority of samples falls in category of magnesium-rich, with a few shifts towards no dominant and calcium regions. The dominance of Magnesium indicates that groundwater is affected by silicate weathering from migmatite and charnockite terrains (Umamageswari et al., 2019). In the anion section, most samples fell in the chloride category, with a few shifting towards bicarbonate, and none being dominant. The dominant chloride indicates an influence on evaporation and agricultural return flow. The water type was  $\text{Ca}^{2+}$ - $\text{Mg}^{2+}$ - $\text{Cl}$ - $\text{SO}_4^{2-}$ , indicating ion exchange and anthropogenic factors (Umamageswari et al., 2019). The piper plot is presented in Fig. 4.

#### 5.2 Gibbs plot

The Gibbs plot indicates that water- rock interaction is the primary factor influencing groundwater chemistry. This is due to silicate weathering from migmatite and charnockite rocks (Sajil Kumar & James, 2013). Some indicate a slight shift due to minimal evaporation effects and suggest that dominant mechanisms, such as mineral dissolution from the host rocks, affect groundwater chemistry (Khan et al., 2020). The Gibbs plot is shown in Fig. 5.

### 6. Irrigation Suitability:

#### 6.1 Wilcox

The Wilcox indicates that 90% of the sample falls in classification of Good - Permissible, and the remaining 5% in Doubtful to Unsuitable and 5% in Unsuitable categories. This indicates that most groundwater is suitable for

irrigation, but some locations may require moderate management depending on the sodium content and salinity. The Wilcox plot is shown in Fig. 6.

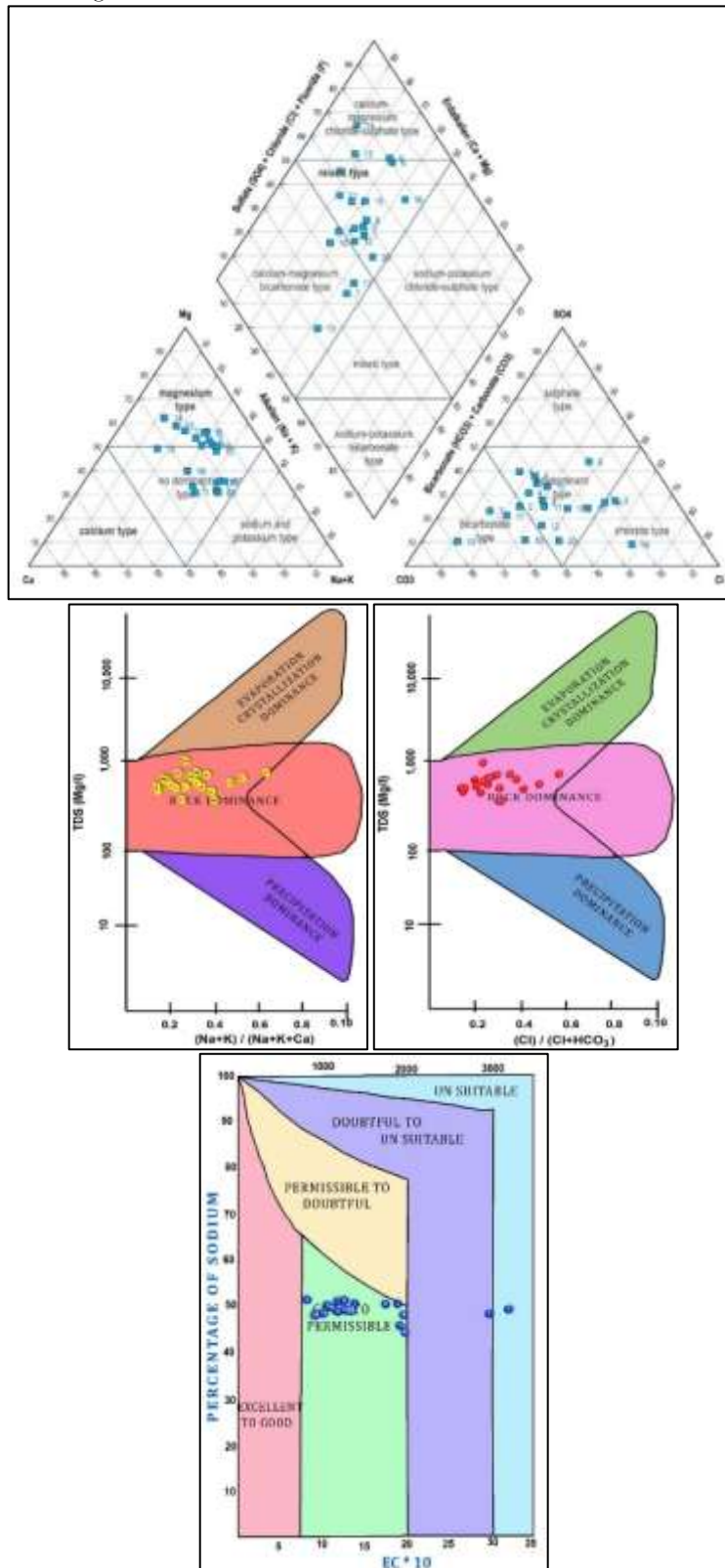


Fig.4) Piper plot, 5)Gibbs plot, 6) Wilcox

### 7. Groundwater Quality Index (GWQI)

The GWQI ranges from 93 to 181, indicating that 95% of samples fall in the category of Poor Water, which can be used for drinking with proper treatment (Table.2). The remaining 5% of the samples in Good Water can be consumed without any treatment (Banerjee et al., 2021).

**Table 2. Classification table for GWQI**

GWQI classification range	Water quality Classification categories	No. of samples	% samples
< 50	Excellent	0	0
50 - 100	Good	1	5
100 - 200	Poor	19	95
200 - 300	Very Poor	0	0
> 300	Unsuitable	0	0
		<b>100</b>	

### 8. Pearson correlation

The Pearson correlation reveals strong positive correlation between TDS & EC  $r = 1$ , indicating that EC is directly proportional to total ionic concentration present in water. The heatmap of Pearson correlation is shown in Fig. 7. This reflects that EC can be used as a reliable proxy for salinity, a pattern commonly observed in groundwater from hard rock terrains. The Total hardness shows strong correlations with calcium  $r = 0.67$  and Magnesium  $r = 0.95$  due to the carbonate and silicate weathering from the hard rock aquifers (Karunanidhi et al., 2014). Calcium is highly correlated with EC and TDS  $r = 0.81$ , indicating that calcium contributes to overall salinity in the calcite dissolution process (Subramani et al., 2005). Sodium shows slight negative correlations with EC  $r = -0.20$  and TDS  $r = -0.20$ , indicating that these originated from the ion exchange or silicate weathering, particularly in low-salinity waters (Karunanidhi, Aravinthasamy, Subramani, et al., 2020). Potassium is weakly correlated with most ions, likely due to adsorption onto clay minerals and low mobility (Karunanidhi et al., 2014). Nitrate shows a weak correlation with all cations and anions, likely from agriculture or wastewater. This aligns with studies from the Chithar River basin (Subramani et al., 2005).

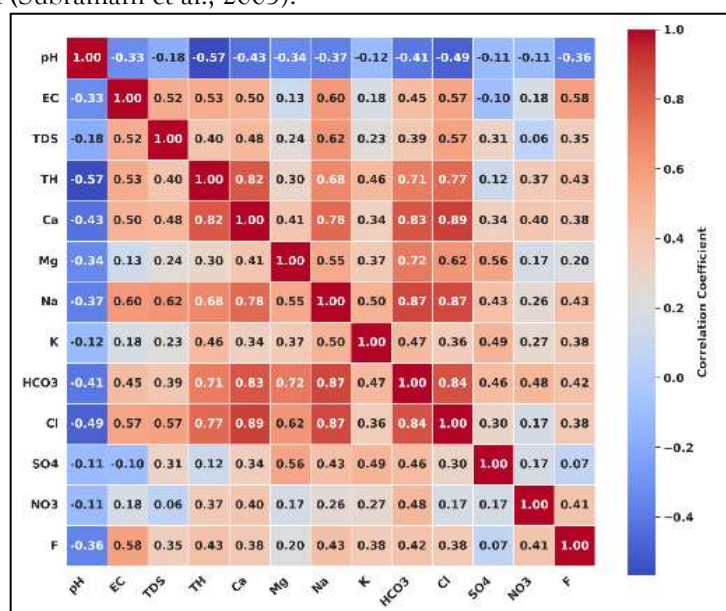


**Fig. 7 Heat map for Pearson correlation**

### 9. Principal Component Analysis (PCA)

PCA was used to identify the sources affecting the groundwater quality in the study area. According to Kaiser's criterion, only PC1 and PC2 had eigenvalues  $>1$ . However, based on the scree plot and to achieve  $>50\%$  variance explanation, four components were retained, indicating 55.34 % of total variance in the datasets, as shown in

Fig. 8a and 8b. PC 1 shows the most significant variance (30.90 %). It is positively loaded with EC (0.905), TDS (0.903),  $\text{Ca}^{2+}$  (0.832), TH (0.826), and  $\text{Mg}^{2+}$  (0.764), and these are typically associated with the dissolution of rock-forming minerals like calcite, dolomite and gypsum. The elevated loadings of EC and TDS indicate increased ionic concentration due to rock-water interactions in hard rock terrains (Ravikumar et al., 2011). PC 1 highlights natural mineral weathering, especially carbonates like Calcium and Magnesium, which increases salinity. PC 2 indicates a positive loading with  $\text{Na}^+$  (0.514) and  $\text{Mg}^{2+}$  (0.367) and negative loadings with  $\text{SO}_4^{2-}$  (-0.599) and  $\text{HCO}_3^-$  (-0.427). These reveal that anthropogenic influences like domestic, ion-exchange processes, and fertiliser use lead to leaching. The moderate presence of  $\text{Na}^+$  and  $\text{Mg}^{2+}$  suggests cation exchange and ion-exchange processes. PC 3 shows high negative loadings with pH (-0.488) and  $\text{NO}_3^-$  (-0.508) and moderate positive loadings on  $\text{Cl}^-$  (0.313) and  $\text{HCO}_3^-$  (0.323). The increased nitrate concentration indicates agricultural contamination, and  $\text{Cl}^-$  (0.313) and  $\text{HCO}_3^-$  (0.323) originated from sewage and soil leaching. The least pH attribute to increased  $\text{CO}_2$  from fertilizer runoff (Ramesh & Elango, 2012). PC 4 has significant negative loadings with  $\text{K}^+$  (-0.459) and  $\text{Cl}^-$  (-0.263) and associated with potash fertilizers, domestic sewage.

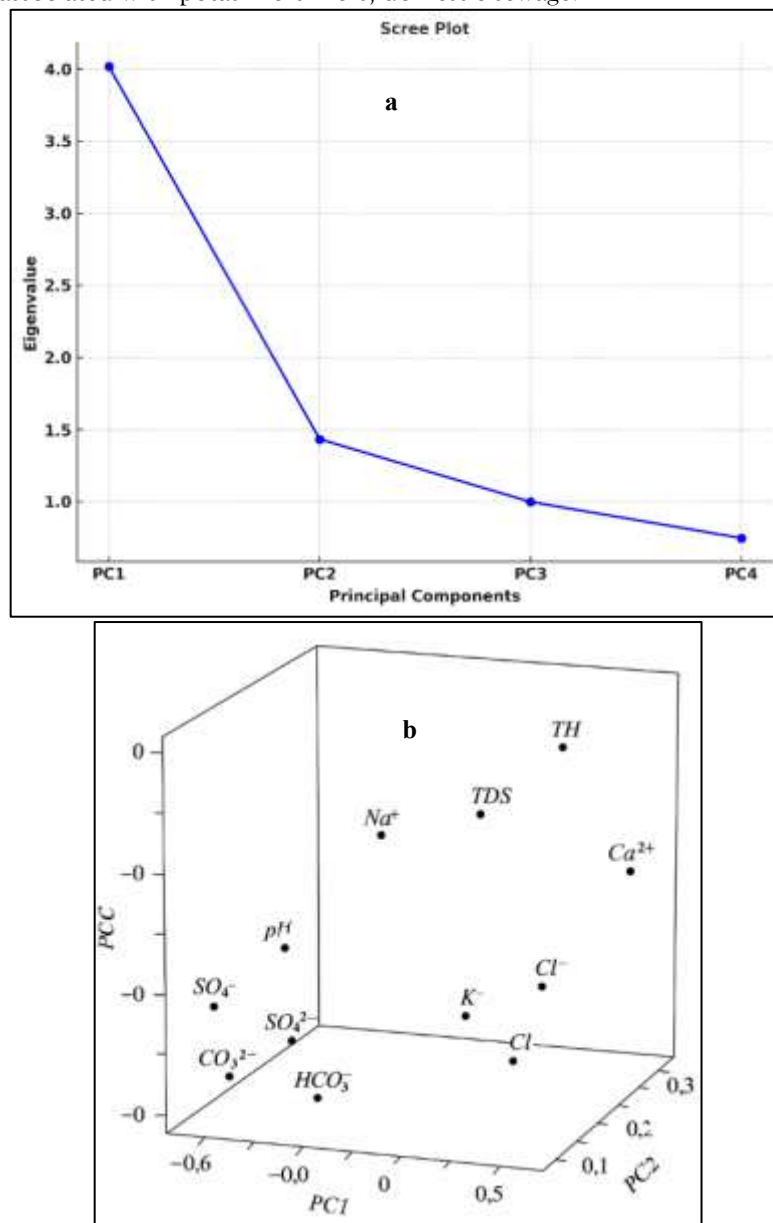


Fig. 8 a) Scree plot , b) 3D cuboid plot of PCA

CONCLUSION:

- The groundwater of the study area is naturally saline and alkaline due to rock-water interactions. Groundwater contamination levels ranks as  $K^+ > TH > EC > HCO_3^- > pH > Mg^{2+} > SO_4^{2-} > TDS > Ca^{2+} > Na^+ > Cl^- > NO_3^-$ , and the dominant water type is  $Ca^{2+} - Mg^{2+} - Cl^- - SO_4^{2-}$  as concluded by the Piper plot.
- The Gibbs diagram indicates groundwater chemistry is primarily driven by rock-water interaction, which contributes to ion dissolution and evaporation, concentrating water salts. Wilcox classification shows that 90% of samples in Good category - Permissible category and very few in doubtful & unsuitable category.
- For drinking purposes, the groundwater quality index indicates that 95% of water is in the poor category and must be consumed after proper treatment. Pearson correlation highlights that EC and TDS were strongly correlated and used as a proxy for salinity in hard rock aquifers. Overall, it indicates rock-water interaction and anthropogenic effects.
- PCA indicates that natural geogenic processes like mineral weathering influence groundwater (PC 1). PC 2 - 4 indicates anthropogenic activities like agricultural runoff, ion exchange & sewage contamination.
- 

### Declarations

“**Funding:** This research has not received any funding from any source.”

“**Conflict of interest:** The authors declare no competing interests.”

**Author contributions:** Pragadeeshwaran Kannan: Conceptualisation, Methodology, Investigation, Data interpretation, Writing – Original draft preparation. Gurugnanam Balasubramaniyan: Supervise, validate, review, and Edit. Bairavi Swaminathan: Software, Map correction. Bagyaraj Murugesan: Map preparation, Review and Editing. Karunanidhi Duraisamy: Review and Writing. All authors read and approved the final manuscript.

**Data availability:** The data supporting the findings of this study are available from the corresponding author upon reasonable request.

### REFERENCES

1. (CGWB), C. G. W. B. (2024). *National Compilation on Dynamic Ground Water Resources of India, 2024*. Ministry of Jal Shakti, Government of India. <https://cgwb.gov.in/cgwbpm/public/uploads/documents/17357169591419696804file.pdf>
2. Adimalla, N., & Qian, H. (2019). Hydrogeochemistry and fluoride contamination in the hard rock terrain of central Telangana, India: analyses of its spatial distribution and health risk. *SN Applied Sciences*, 1(3), 202.
3. Adithya, V. S., Chidambaram, S., Thivya, C., Thilagavathi, R., Prasanna, M. V., Nepolian, M., & Ganesh, N. (2016). A study on the impact of weathering in groundwater chemistry of a hard rock aquifer. *Arabian Journal of Geosciences*, 9, 1-11.
4. Ahirvar, B. P., Kumar, R., & Das, P. (2023). *Hydrogeo-chemical characteristics of groundwater and seasonal variation in coal mining area, Madhya Pradesh, India*.
5. American Public Health Association. (2017). *Standard Methods for the Examination of Water and Wastewater*.
6. Banerjee, K., Santhosh Kumar, M. B., Tilak, L. N., & Vashistha, S. (2021). Analysis of groundwater quality using GIS-based water quality index in Noida, Gautam Buddh Nagar, Uttar Pradesh (UP), India. *Applications of Artificial Intelligence and Machine Learning: Select Proceedings of ICAAIML 2020*, 171-187.
7. Choi, K., & Chong, K. (2022). Modified Inverse Distance Weighting Interpolation for Particulate Matter Estimation and Mapping. In *Atmosphere* (Vol. 13, Issue 5). <https://doi.org/10.3390/atmos13050846>
8. Duraisamy, S., Govindhaswamy, V., Duraisamy, K., Krishinaraj, S., Balasubramanian, A., & Thirumalaisamy, S. (2019). Hydrogeochemical characterization and evaluation of groundwater quality in Kangayam taluk, Tirupur district, Tamil Nadu, India, using GIS techniques. *Environmental Geochemistry and Health*, 41, 851-873.
9. Karunanidhi, D., Aravinthasamy, P., Deepali, M., Subramani, T., & Roy, P. D. (2020). The effects of geochemical processes on groundwater chemistry and the health risks associated with fluoride intake in a semi-arid region of South India. *RSC Advances*, 10(8), 4840-4859.
10. Karunanidhi, D., Aravinthasamy, P., Subramani, T., Roy, P. D., & Srinivasamoorthy, K. (2020). Risk of fluoride-rich groundwater on human health: remediation through managed aquifer recharge in a hard rock terrain, South India. *Natural Resources Research*, 29, 2369-2395.
11. Karunanidhi, D., Vennila, G., Suresh, M., & Karthikeyan, P. (2014). Geoelectrical Schlumberger investigation for characterizing the hydrogeological conditions using GIS in Omalur taluk, Salem District, Tamil Nadu, India. *Arabian Journal of Geosciences*, 7, 1791-1798.
12. Khan, A. F., Srinivasamoorthy, K., & Rabina, C. (2020). Hydrochemical characteristics and quality assessment of groundwater along the coastal tracts of Tamil Nadu and Puducherry, India. *Applied Water Science*, 10(2), 74. <https://doi.org/10.1007/s13201-020-1158-7>
13. Panneerselvam, B., Muniraj, K., Duraisamy, K., Pande, C., Karuppanan, S., & Thomas, M. (2023). An integrated approach to explore the suitability of nitrate-contaminated groundwater for drinking purposes in a semiarid region of India. *Environmental*

*Geochemistry and Health*, 45(3), 647–663.

14. Panneerselvam, B., Paramasivam, S. K., Karuppannan, S., Ravichandran, N., & Selvaraj, P. (2020). A GIS-based evaluation of hydrochemical characterisation of groundwater in hard rock region, South Tamil Nadu, India. *Arabian Journal of Geosciences*, 13, 1–22.
15. Rajmohan, N., & Elango, L. (2005). Nutrient chemistry of groundwater in an intensively irrigated region of southern India. *Environmental Geology*, 47, 820–830.
16. Rajmohan, N., & Elango, L. (2006). Hydrogeochemistry and its relation to groundwater level fluctuation in the Palar and Cheyyar river basins, southern India. *Hydrological Processes: An International Journal*, 20(11), 2415–2427.
17. Ramesh, K., & Elango, L. (2012). Groundwater quality and its suitability for domestic and agricultural use in Tondiar river basin, Tamil Nadu, India. *Environmental Monitoring and Assessment*, 184, 3887–3899.
18. Ravikumar, P., Somashekar, R. K., & Angami, M. (2011). Hydrochemistry and evaluation of groundwater suitability for irrigation and drinking purposes in the Markandeya River basin, Belgaum District, Karnataka State, India. *Environmental Monitoring and Assessment*, 173(1), 459–487.
19. Sajil Kumar, P. J., & James, E. J. (2013). Physicochemical parameters and their sources in groundwater in the Thirupathur region, Tamil Nadu, South India. *Applied Water Science*, 3, 219–228.
20. Stachelek, J., & Madden, C. J. (2015). Application of inverse path distance weighting for high-density spatial mapping of coastal water quality patterns. *International Journal of Geographical Information Science*, 29(7), 1240–1250. <https://doi.org/10.1080/13658816.2015.1018833>
21. Subramani, T., Elango, L., & Damodarasamy, S. R. (2005). Groundwater quality and its suitability for drinking and agricultural use in Chithar River Basin, Tamil Nadu, India. *Environmental Geology*, 47, 1099–1110.
22. Subramaniyan, A., Balaji, A., & Andimuthu, R. (2024). Assessment of groundwater quality for drinking and irrigation in Dindigul district, southern India: Hydrochemical characterization and spatial analysis. *Desalination and Water Treatment*, 320, 100772. <https://doi.org/10.1016/J.DWT.2024.100772>
23. Tyagi, S., Sharma, B., Singh, P., & Dobhal, R. (2013). Water quality assessment in terms of water quality index. *American Journal of Water Resources*, 1(3), 34–38.
24. Umamageswari, T. S. R., Sarala Thambavani, D., & Liviu, M. (2019). Hydrogeochemical processes in the groundwater environment of Batlagundu block, Dindigul district, Tamil Nadu: conventional graphical and multivariate statistical approach. *Applied Water Science*, 9(1), 14.
25. Upendra, B., Ciba, M., Aiswarya, A., Dev, V. V., Sreenivasulu, G., & Krishnan, K. A. (2022). Mechanisms controlling the dissolved load, chemical weathering and CO<sub>2</sub> consumption rates of Cauvery River, South India: role of secondary soil minerals. *Environmental Earth Sciences*, 81(3), 103.
26. Wang, G., Wu, J., Zhai, X., Zhang, H., & Bi, Y. (2022). Temporal variation of hydrogeochemical characteristics and processes of aquifers in the Liuqiao coal mine. *Energy Exploration & Exploitation*, 40(5), 1382–1393.
27. WHO. (2017). *Guidelines for drinking-water quality: fourth edition incorporating first addendum* (4th ed., 1). World Health Organization. <https://iris.who.int/handle/10665/254637>